

THE DEVELOPMENT OF A VELOCITY PREDICTION PROGRAM FOR TRADITIONAL DUTCH SAILING VESSELS OF THE TYPE SKÛTSJE

Pepijn de Jong¹
Michiel Katgert²
Lex Keuning³

ABSTRACT

A Velocity Prediction Program has been developed for the verification of the handicap rule used for sailing races with traditional Dutch sailing vessels of the type skûtsjes. To make this VPP suitable for this type of vessels model experiments in the towing tank and the wind tunnel have been performed and the resulting formulations for the hydromechanic and aerodynamics are integrated into a specially tailored VPP.

The paper presents the background of the hydromechanic and aerodynamic models and the inner workings of the resulting VPP. Results are shown for the comparison of performance of the competing vessels on pre-defined racing course for a number of wind velocities.

The paper concludes that the newly developed VPP is found to be suitable to quantify the performance differences between the boats it is aimed for and in such way can be used as a tool to verify and when necessary improve the handicap rule currently used.

1. INTRODUCTION

A frequently returning theme in sail racing with yachts that are not part of a one design class is the creation of a handicap system that is deemed fair by all competitors. The idea behind such a system is that in the race results the capabilities of the crews are only accounted for and not, as is the case with the plain race results, the technical capabilities of the yachts. For such a system basically two main solutions exist:

1. The correction of the racing time for technical differences between the competing yachts;
2. The technical adaptation of the yachts, such that their theoretical performance, without the influence of the crew, is equivalent.



Figure 1 Skûtsje

¹ Assistant Professor, Ship Hydromechanics Laboratory, Delft University of Technology

² Researcher, Ship Hydromechanics Laboratory, Delft University of Technology

³ Associate Professor, Ship Hydromechanics Laboratory, Delft University of Technology

Of both methods, the latter can be much harder to achieve when there are large differences between the competing sailing yachts. Both solutions require adequate knowledge of the theoretical performance of the participating yachts. One way of obtaining this information is by using a so called Velocity Prediction Program or VPP. A VPP is a computer program that can calculate the sailing performance of a sailing yacht by linking an aerodynamics model for the sailing forces with a hydromechanics model for the resistance, stability and lifting forces on the yacht's hull. Both computational models usually are obtained by model experiments, in wind tunnel for the sailing forces and in the towing tank for the resistance. Usually these experiments are generic and by using systematical parameter variations (of the geometry, the weight, and the weight distribution) it is possible to describe the characteristics of all yachts involved.

In the north of the Netherlands the SKS (Sintrale Kommissje Skûtsjesilen) sail races are held yearly. In these races 14 syndicates, using *skûtsjes*, compete in a yearly organized race series, each syndicate often representing a city or a village. *Skûtsjes* are traditional Frisian sailing vessels from the start of the 20th century, and form a subtype of the Dutch tjalk. These vessels were originally used for cargo transport in the inland waters of Frisia. They are flat-bottomed and carry shallow rounded leeboards on their sides that are used as a substitute for the keel. Their length is about 15 to 20 meters; they are 3.5 to 4 meters wide and have a draft of only around 0.4 meter. Their rig is of the sloop type, with a short curved gaff of about a third of the boom length and a stay sail. Figure 1 shows a skûtsje as used in the SKS races.

To keep the SKS races attractive for the public a fairly basic handicap system is used. This system attempts to equalize the sailing performance of the 14 different skûtsjes, by limiting the amount of sail that can be used for each vessel. The result is that the actual finish equals the race result. The maximum allowed sailing area is prescribed by a simple formula, based on the main dimensions of the vessels:

$$SA = 2.15 \cdot L_{wl} \cdot [B_{wl} + 2T] \quad (1)$$

The formula has most recently been revised in 2000; hence it is referred to as Formula 2000. At the time of this revision an evaluation was foreseen several years later. During this evaluation the SKS felt the need to perform an in depth study to verify the formula. For this reason the SKS contracted the Kenniscentrum Jachtbouw (a knowledge center for the yachting industry of the Noordelijke Hogeschool Leeuwarden - NHL). The NHL subcontracted the Ship Hydromechanics Laboratory of Delft University of Technology to devise a Velocity Prediction Program specifically tailored for skûtsjes. This VPP is created to enable the NHL to study the effectiveness of the Formula 2000, and to provide theoretical support when devising a new formula in case this is deemed necessary. Besides the TUDelft, the Maritime Research Institute Netherlands was subcontracted for performing full scale resistance tests and Anmar Engineering for measurement of the hulls to obtain lines plans of each boat and for performing stability tests.

The current paper describes the development of this VPP specifically tailored for skûtsjes. In the next section the general approach of the research project is laid out. The following sections detail respectively the resistance model, the stability, the aerodynamic model, and the VPP solver and optimizations. Finally results are presented for the comparison between the 14 skûtsjes. The final section summarizes the conclusion.

2. APPROACH

To set up the VPP three aspects of the vessels are combined:

1. The resistance and side force production (resistance model, described in section 3)
2. The stability and volume of displacement (section 4)
3. The sail forces (aerodynamic model, described in section 5)

The first aspect is covered by the resistance model as detailed in section 3. In this case model experiments in the towing tank are used to obtain resistance data at a number of forward speeds and geometrical variations (trim, drift, heeling, leeboard angle and rudder angle). Due to budgetary restrictions only four boats were selected to carry out the towing tank tests. These models were selected to cover the most important parameter variations in the group of 14 boats. With one of the four a full set of measurements were carried out to obtain polynomial expressions for the influence of the geometric variations due to trim,

heeling and drift. With the other three a more limited test program was carried out to obtain polynomial expressions for the influence of the hull form on the upright and heeled resistance.

This approach enabled obtaining a resistance model at limited cost, while providing as much information as possible for the range of 14 boats. The approach was deemed justifiable, especially due to the fact that the VPP was aimed at quantifying the differences in performance between 14 relatively similar boats, and not at obtaining an absolute performance indication nor at addressing performance differences between very dissimilar designs.

For the water depth 2.5 m full scale was chosen. This value deemed to be representative of the water depth in which the races are performed. Due to the restricted water depth, the resistance of the boats is highly influenced and will steeply increase when the boat speed increases. The model experiments were setup with limiting value of the Froude number over the depth of 0.8, as beyond this velocity the resistance will steeply increase due to shallow water effects.

The second aspect, the stability, is determined by the hull shape and the height of the center of gravity. Both were unknown and therefore all vessels have been measured to construct a digital lines plan and stability tests have been performed to obtain the position of the center of gravity. This is detailed in section 4.

The third aspect, the sail forces or the aerodynamic model, has been dealt with in two ways. Within the original budget, there was no room for additional wind tunnel testing. Therefore, the sail force model was initially based on wind tunnel tests previously carried out and published. In particular use was made of the sail coefficients obtained in the so-called Indosail project. In the 80s of the last century numerous wind tunnel tests were carried out with different sail types by HSVA. The results have been partially reproduced by Indesteege (1989).

At a later stage, due to fortunate circumstances the possibility arose to perform wind tunnel tests with a model of one of the 14 skûtsjes. Although no geometric variations were possible in these limited tests, a much more realistic sail model was obtained, which was used to significantly enhance the VPP. This latter model is presented in the current paper. The sail force model will be detailed in section 5.

Finally, these three aspects were combined with a solver routine to form the VPP. The results of this VPP can be used to obtain the time per sailed mile on a predefined track to compare the results of 14 boats, as well as to evaluate possible measures to equalize the sailing performance.

As the model is setup with limited budget and as a means to compare the relative performance of the boats the effort has been directed at adequately describing the differences between the skûtsjes and not so much at achieving absolute performance predictions. The latter would require a much higher level of detail and in turn much more extensive and costly model experiments.

3. RESISTANCE MODEL

3.1. Model selection

As stated, due to budgetary restrictions only four boats could be selected for the towing tank tests. To get an idea which parameters of these boats mostly determine the residuary resistance characteristics of this type of ships, regression analysis was carried out on the resistance results of similar traditional vessels, tested earlier at the Ship Hydromechanics Laboratory. It was found that the following parameters and the relation them were most important for the specific residuary resistance:

- Length waterline
- Width waterline
- Draft
- Waterline area
- Lengthwise position of the center of buoyancy

While studying the main particulars of the 14 skûtsjes, no. 10 (widest and shallow), no. 2 (most narrow, almost shortest and deepest), no. 14 (longest and wide), and no. 12 (waterline area) were selected to perform towing tank measurements with.

| | Lwl | Bwl | T | D | ∇ | S | SA | ZCE | GM |
|----|-------|------|------|------|----------------|----------------|----------------|------|------|
| | m | m | m | m | m ³ | m ² | m ² | m | m |
| 1 | 17.29 | 3.51 | 0.43 | 0.79 | 17.42 | 62.80 | 163.7 | 6.88 | 1.68 |
| 2 | 17.30 | 3.36 | 0.45 | 0.68 | 17.45 | 62.39 | 156.1 | 6.77 | 1.69 |
| 3 | 17.43 | 3.78 | 0.42 | 0.81 | 19.83 | 68.11 | 168.4 | 7.18 | 2.01 |
| 4 | 17.44 | 3.59 | 0.41 | 0.75 | 18.32 | 65.81 | 168.4 | 7.14 | 2.00 |
| 5 | 17.46 | 3.58 | 0.45 | 0.79 | 18.63 | 64.56 | 165.8 | 6.99 | 1.89 |
| 6 | 17.48 | 3.57 | 0.38 | 0.81 | 16.98 | 63.68 | 165.0 | 6.99 | 1.93 |
| 7 | 17.51 | 3.47 | 0.43 | 0.75 | 17.71 | 63.10 | 162.0 | 6.79 | 1.76 |
| 8 | 17.55 | 3.48 | 0.43 | 0.76 | 17.87 | 63.68 | 162.6 | 6.70 | 1.75 |
| 9 | 17.57 | 3.48 | 0.41 | 0.69 | 16.38 | 61.48 | 160.2 | 6.55 | 1.87 |
| 10 | 17.69 | 3.92 | 0.38 | 0.75 | 18.61 | 68.49 | 177.9 | 7.45 | 2.46 |
| 11 | 17.70 | 3.46 | 0.45 | 0.8 | 18.13 | 63.80 | 161.3 | 7.02 | 1.61 |
| 12 | 17.75 | 3.68 | 0.40 | 0.85 | 18.63 | 68.04 | 168.8 | 7.15 | 2.17 |
| 13 | 17.79 | 3.61 | 0.40 | 0.71 | 17.26 | 64.12 | 168.0 | 6.92 | 2.01 |
| 14 | 17.89 | 3.72 | 0.40 | 0.83 | 17.91 | 68.39 | 170.4 | 7.42 | 2.39 |

Table 1 Main particulars of the SKS fleet

3.2. Test setup

The experiments were performed in towing tank #2 of the Ship Hydromechanics Laboratory of the TUDelft. This tank measures 75 m in length and 2.75 m in width. The testing was performed at a model scale of 1:9. The reason to choose the smaller towing tank was the limited water depth of 2.5 m full scale, equivalent to 0.278 m on model scale.

The models were tested accordingly the standard testing procedure of the Ship Hydromechanics Laboratory of the TUDelft. The models were free to heel, sink and trim by using two vertical balance arms. The trimming moment was applied by transferring a weight over longitudinal rails on the model. The heeling angle was applied by moving this same weight transversely on an electrical driven worm drive and using an accurate spirit level. The drift angle was applied by transversely moving the forward balance leg. The resistance force was measured by attaching the tow-string to a force transducer and on both balance arms force transducers were mounted to measure the side force and the yaw moment. Trim and sinkage were determined with two potentiometers in the balance arms.

Turbulence stimulation was achieved by using strips of carborundum particles attached to the model at three stations. The additional resistance of these strips was corrected for by first performing test with single width carborundum strips and subsequently with double width strips and recording the difference in resistance.



Figure 2 Test setup, three single width carborundum strips are visible near the bow

All measured signals were amplified and filtered with a low-pass filter with a cut-off frequency of 5 Hz. The signal was passed via an A/D-converter to the data recording PC. The signals were zeroed. The runs were about 20 seconds in length. Figure 2 shows the test setup.

3.3. Test program

All four models were subjected to a limited test program, while model 14 was more extensively tested.

The limited testing program consisted of tests for the upright resistance for a Froude number range from 0.1 to 0.3 at three different trimming moments. These trimming moments were applied to correct for the difference in height of the attachment point of the tow string and the height of the center of effort of the sail forces. Besides the upright resistance also the resistance at 15 degrees heeling angle for the same speed range was measured. No leeboard was mounted during these tests and the rudder was fixed at 0 degrees rudder angle.

The upright resistance was measured twice for each forward speed; once with single width carborundum strips and once with double width strips to account for the increased resistance due to the strips.

Model 14 was subjected to a more extensive program, according to the standard testing method of sailing yachts of the Ship Hydromechanics Laboratory. Three forward speeds (Fn 0.1, 0.2, and 0.3), four heeling angles (0, 10, 15, and 20 degrees), three leeway angles (0, 6, and 9 degrees), and two rudder angles (0 and 10 degrees) were tested. The leeboard was mounted and fixed in the maximum submerged orientation. This orientation was limited by the relatively small water depth to 0.27 m.

3.4. Data processing

The measured resistance was corrected for the influence of the carborundum strips and subsequently extrapolated using Froude's method. The resistance was split into a viscous part and a residuary part. The viscous part was determined by applying the ITTC-57 friction line for both model scale and full scale and using a form factor of 1.20 obtained with the method of Prohaska. The residuary part was extrapolated by applying the scale factor α^3 , where α is the linear geometric scale factor.

3.5. Hydromechanic model

The hydromechanic model has been setup in accordance with work carried out in the Ship Hydromechanics Laboratory in conjunction with the Delft Systematic Yacht Hull Series as published by Gerritsma et al. (1981) and (1988) and Keuning et al. (1996), (1997) and (1998).

Resistance of bare hull with rudder

The viscous resistance can be calculated using the ITTC-57 friction line and the form factor found from the model experiments:

$$R_v = \frac{1}{2} \rho V^2 S C_{f \text{ ITTC-57}} (1+k)$$

$$C_{f \text{ ITTC-57}} = \frac{0.075}{(\log(Rn) - 2)^2} \quad (2)$$

$$Rn = \frac{VL}{\nu}$$

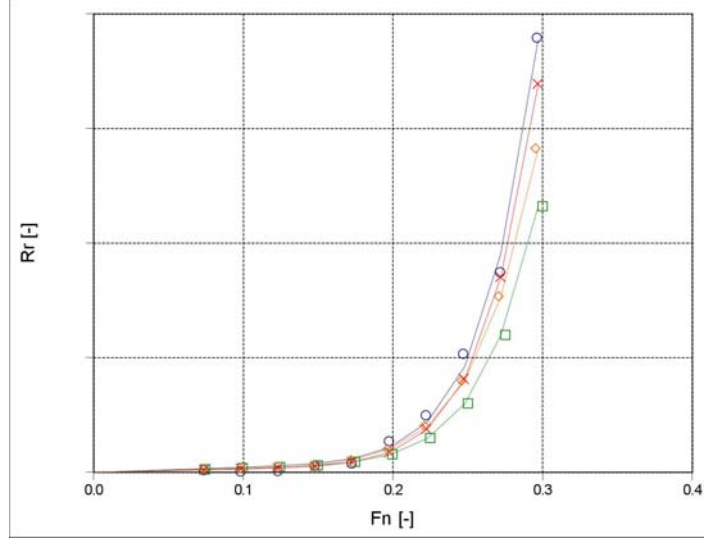


Figure 3 Residuary resistance measured (points) and modeled (solid lines)

For the upright residuary resistance of the bare hull with rudder a polynomial expression has been determined using the upright resistance experiments of the four models. The coefficients a_0 to a_3 are dependent on the Froude number.

$$\frac{R_r}{\nabla \rho g} = a_0 + a_1 \frac{B_{wl}}{L_{wl}} + a_2 \frac{B_{wl}}{T} + a_3 \frac{L_{wl}}{\nabla^{1/3}} \quad (3)$$

Figure 3 shows a comparison of the measured residuary resistance for these four models and the residuary resistance calculated with equation(3).

Extra resistance due to trim

The residuary resistance of the bare hull has been determined for trimming moments of 51 kNm and 115 kNm. The resistance force at 115 kNm can be described with a similar polynomial expression, with a different set of coefficients b_0 to b_3 :

$$\frac{R_{r\theta 115}}{\nabla \rho g} = b_0 + b_1 \frac{B_{wl}}{L_{wl}} + b_2 \frac{B_{wl}}{T} + b_3 \frac{L_{wl}}{\nabla^{1/3}} \quad (4)$$

Moreover, it has been found that the extra residuary resistance at 51 kNm is 25% of that of 115 kNm. Now the extra resistance due to a trimming moment can be found with:

$$\Delta R_{r\theta} = factor \cdot (R_{r\theta 115} - R_r) \quad (5)$$

Where factor is a quadratic interpolation function that is 0 for $M_{trim} = 0$, 0.25 for $M_{trim} = 51$ kNm, and 1 for $M_{trim} = 115$ kNm.

Extra resistance due to heel

The change of resistance due to heel consists of a change in frictional resistance due to the changed wetted surface (6) and a change of residuary resistance determined during the experiments at 15 degrees heeling angle (7). The latter can again be described with a similar expression as previously found, now with coefficient set c_0 to c_3 .

$$\Delta R_{f\theta} = \frac{1}{2} \rho V^2 C_f (S_\phi - S) \quad (6)$$

$$\frac{\Delta R_{r\phi 15^\circ}}{\nabla \rho g} = c_0 + c_1 \frac{B_{wl}}{L_{wl}} + c_2 \frac{B_{wl}}{T} + c_3 \frac{L_{wl}}{\nabla^{1/3}} \quad (7)$$

The residuary resistance due to heel at the correct heeling angle is found by linear interpolation:

$$\Delta R_{r\phi} = \frac{\phi}{15} \Delta R_{r\phi 15^\circ} \quad (8)$$

Induced resistance

The induced resistance has been determined with the extensive measurements performed with model 14. The induced resistance, the resistance associated with the side force production generated by bare hull, rudder, and leeboard traveling at a leeway angle. The induced resistance is determined adopting the method of the Delft Systematic Yacht Hull Series, using the so-called effective draft T_e . This method has been detailed by Keuning and Sonnenberg (1998).

$$R_i = \frac{F_h^2}{\pi T_e^2 \frac{1}{2} \rho V^2} \quad (9)$$

The effective draft was determined for from the measurements for two situations:

1. Maximum leeboard submergence, limited by the water depth (set at 2.5 m). This is used when sailing close hauled to beam reaching, when significant side force is generated by the sails.
2. Minimum leeboard submergence. The leeboard is covered by the hull and does not contribute to the side force production. This case occurs when broad reaching to dead running.

For both cases the effective draft has been determined and tabulated dependent on heeling angle and forward speed. The dependence on forward speed is weak; however, the effective draft is strongly dependent on the heeling angle and becomes larger when the heeling angle increases. This can be attributed to end plate effects due to the proximity of the floor, that become stronger when the heeling angle increases, decreasing the distance between the leeboard tip and the floor.

Leeboard resistance

The total leeboard resistance does not equal zero when it is not producing side force. The remaining resistance consists of frictional, form, and residuary components. Due to its small waterline area the residuary component of the leeboard resistance was assumed negligible. Then the leeboard resistance was assumed equal to the frictional resistance determined with the ITTC-57 friction line. Any deviation from this friction line and the actual measured leeboard resistance (measured with the presence of the hull) is discounted in the form factor. It should be noted that this approach is very coarse. Interaction effects are ignored and the wave making resistance is, although very small, scaled incorrectly with the viscous resistance.

$$R_{leeboard} = \frac{1}{2} \rho V^2 C_{f \text{ ITTC-57}} S_{leeboard} (1+k) \quad (10)$$

Total resistance

The total resistance is found by addition of the previously detailed components:

$$R_t = R_r + R_v + \Delta R_{r\theta} + \Delta R_{r\phi} + \Delta R_{f\phi} + R_i + R_{leeboard} \quad (11)$$

4. STABILITY

The stability, volume of displacement and along with that the centers of gravity and buoyancy were acquired by measuring the lines plans of all 14 skûtsjes and performing stability tests. All boats have been built around 1900 and over the years have undergone numerous changes, damages and repairs, making any

available lines drawing obsolete. Especially over the last years most of the boats have been extended to the maximum length possible within the originality regulations.

Each boat has been taken out of the water and measured by using a semi automatic technique to obtain the frames and center vertical by Annmar Engineering, as published by Wagenaar (2008). Even then it took significant effort with 3D modeling software to obtain reasonable 3D lines drawings of each boat. Still then numerous irregularities and asymmetries were present, often due to damages and repairs. The lines drawings used for the models have been averaged over port and starboard side. All this leads to a difficult to quantify geometrical uncertainty.

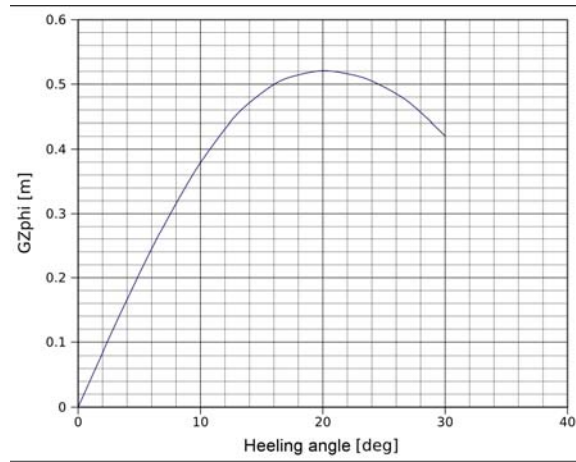


Figure 4 Arms of stability

With the resulting lines drawings and the heights of the center of gravity the curves of arms of stability can be constructed. These curves are used in the VPP to calculate the heeling moment at a given heeling angle. Figure 4 shows a typical curve of arms of stability. The relative small angle of maximum stability is apparent and is due to the fact that the stability of these vessels is for the largest part based on the form stability and not due to a low center of gravity. This stems from the absence of a ballasted keel.

5. AERODYNAMIC MODEL

5.1. Wind model

A wind gradient is assumed based on the wind velocity given at 10 meters above the water level. To calculate the wind velocity at the height of the center of effort ZCE equation (12) is used.

Figure 5 Arms of stability

$$wndgrad = \left(\frac{ZCE \cdot \cos(\varphi)}{10} \right)^{0.1} \quad (12)$$

The sine and cosine components of the true wind velocity become, where α_{tw} is the true wind angle, φ the heeling angle and V_{tw} the true wind velocity:

$$\begin{aligned} V_{tw\sin} &= V_{tw} \sin(\alpha_{tw}) \cdot wndgrad \cdot \cos(\varphi) \\ V_{tw\cos} &= V_{tw} \cos(\alpha_{tw}) \cdot wndgrad \end{aligned} \quad (13)$$

In this equation the cosine of the heeling angle is assumed to include the influence of the heeling angle on apparent velocity and the sailing forces. Finally the apparent wind velocity and angle can found as:

$$V_{aw} = \sqrt{(V_s + V_{tw\cos})^2 + V_{tw\sin}^2}$$

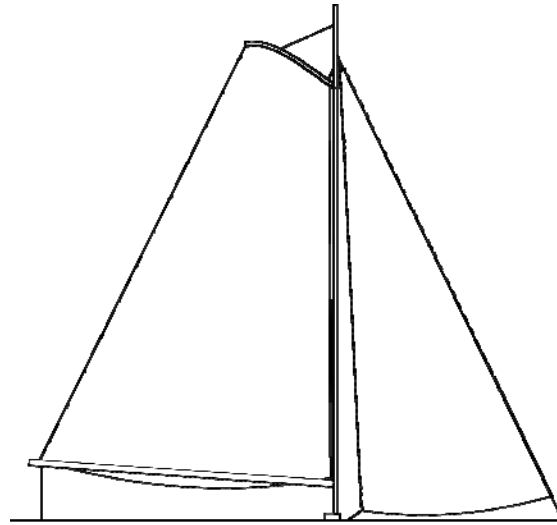
$$\alpha_{aw} = \arctan\left(\frac{V_{tw\sin}}{V_s + V_{tw\cos}}\right) \quad (14)$$

5.2. Sail model

Test setup

For the wind tunnel measurements the Low-Speed Low-Turbulence Wind Tunnel of the Faculty of Aerospace Engineering of the Delft University of Technology was used. This tunnel is an atmospheric tunnel of the closed throat single return type, with a contraction ratio of 17.8. This tunnel is capable of test section velocities up to 120 m/s. The free stream turbulence level in the test section varies from 0.015% at 20 m/s to 0.07% at 75 m/s. The 10 interchangeable octagonal test sections are 1.80 m wide, 1.25 m high and 2.60 meters long.

The model used was again model 14. A polyurethane foam model was made of the above water part of the hull. The boom, gaff and mast were made of wood and the sails of spinnaker rip-stop nylon. Figure 6 shows a typical rig of a skûtsjes. The scale factor was 1:25, resulting in a model of about 80 cm length and a mast height of 73 cm. The total sail area became 0.273 m², resulting in a maximum blockage of the test section of about 16%.



main sail AR = 2.1 and jib AR = 4.4
Combined AR = 2.9

Figure 6 Typical rig skûtsje

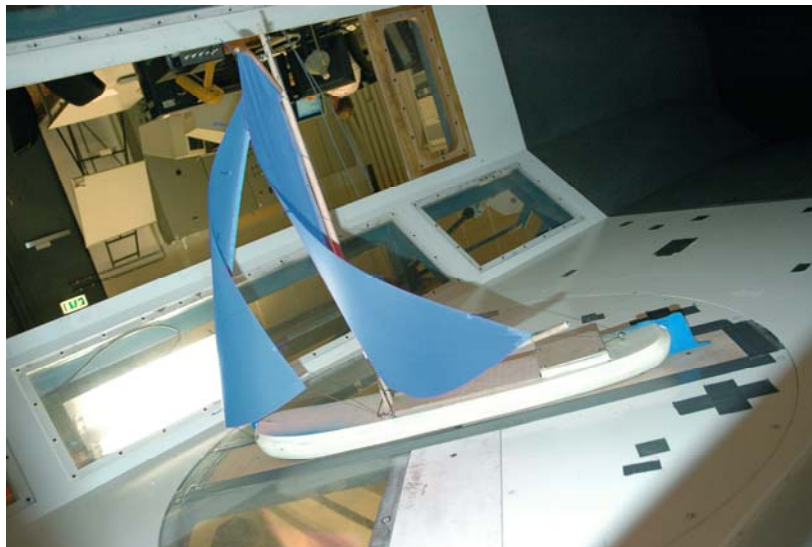


Figure 7 Test setup wind tunnel

The model was attached to a mechanically actuated turn table flush with the tunnel wall allowing the model to be rotated around its vertical axis. The model itself was attached to a force balance system, allowing the accurate measurement of forces and moments on the model in six degrees of freedom. The test setup is depicted in Figure 7.

The data acquisition system recorded the forces and moments on the model, the orientation of the model (the angle of attack), and the flow velocity.

For correct scaling the Reynolds number should be kept constant for model and full scale, resulting in very high flow velocities (full scale wind velocity times the scale factor). Nevertheless, the flow velocity in the wind tunnel is limited by the power of the sheet winches and by the structural strength of the model. Additionally, it would be very hard to find materials for mast and sails that would have similar deformation compared to the full scale materials within the limits of the model geometry.

For that reason, the velocity for sail testing in wind tunnels usually is kept much lower and the inaccuracies due to the incorrect scaling are taken for granted. The only way of restricting dissimilarity between model and full scale is using larger models. A flow velocity of 7 m/s was found to be feasible for the test setup. At larger flow velocities the deformation of mast and sails became unrealistically large.

A boundary layer profile of the flow on the model was achieved by mounting the model flush on the tunnel wall. Generally for wind tunnel experiments a very thin boundary layer is required. For this reason most facilities are designed to minimize the boundary layer thickness. For the wind tunnel tests presented here the boundary layer profile was assumed to have the same shape and relative thickness as its full scale equivalent. The velocity gradient has not been verified.

In real life a ship sailing at forward speed will encounter a different apparent wind velocity and apparent wind angle at different heights above the water level, due to the velocity gradient. This is known as twist. No twist stimulation has been performed for the wind tunnel experiments.

The wind tunnel boundaries have additional effects on the flow about the model. Rea and Pope (1984) separate three distinct effects:

1. Lateral constraint to the flow pattern around the body, solid blockage, leading to an increase of the flow velocity around the body.
2. Lateral constraint to the flow pattern around the wake, wake blockage, again leading to an increase of the flow velocity around the body.
3. Alteration to the curvature of the flow due to lifting devices due the tunnel walls, leading to an increase in angle of attack.

These three influences are discounted in the measured data.

Testing procedure

As stated, a flow velocity of 7 m/s was chosen. The driving force, heeling force, and heeling moment were measured for a range of apparent wind angles of 10 (close hauled) to 180 (running ahead) degrees at intervals of 2 degrees upwind and of 5 and 10 degrees downwind. At each apparent wind angle the sheeting of jib and main sail was adjusted to yield the maximum driving force. With this sail setting fixed the apparent wind angle was adjust to +4, +2, -2, and -4 degrees. At all 5 points the forces and moments were measured, along with the flow velocity and air density to obtain the force and moment coefficients.

Additionally, the bare poles forces at the same range of apparent wind angles were measured.

Data processing and results

The bare pole forces were subtracted from the full sail set forces. Subsequently, the force and moment coefficients were corrected for the three blockage effects and the enveloping curve was found for the maximum driving force for each apparent wind

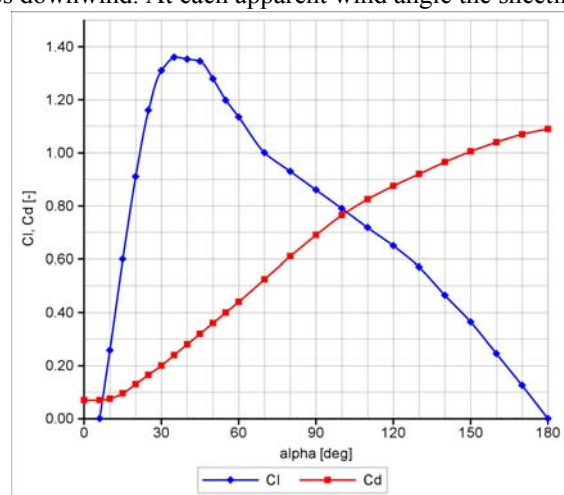


Figure 8 Aerodynamic lift and drag coefficients

angle.

The lift and drag curves were constructed by selecting the corresponding points on the heeling force curve and conversion of each driving force-heeling force pair to lift and drag. The resulting curves were slightly faired. The faired data is depicted in Figure 8. At large apparent wind angles (larger than 150 degrees) deviations were visible between the raw and faired data. These were caused by the irregular behavior of the jib that was partially covered by the main sail. In the faired data this effect has been removed.

Sail model

The faired lift coefficient determined above has been used directly in the sail model and is designated C_{l0} . The drag has been further processed, in order to implement dependence of the rig on the rig dimensions. In particular dependence on the aspect ratio has been added. Therefore, the drag has been separated in several components:

$$C_d = C_{d0} + C_{ds} + C_{di} + C_{dhull} + C_{drigging} \quad (15)$$

The induced drag is determined by:

$$C_{di} = \frac{C_l^2}{\pi AR_e} \quad (16)$$

With AR_e the effective aspect ratio of the rig, equaling the geometric aspect ratio times a efficiency factor e . This factor has been found by fitting the slope of the $C_l^2 - C_d$ -graph (refer to Figure 9) for small angles of attack. Using this approach, a value of 2 has been found for the efficiency factor e .

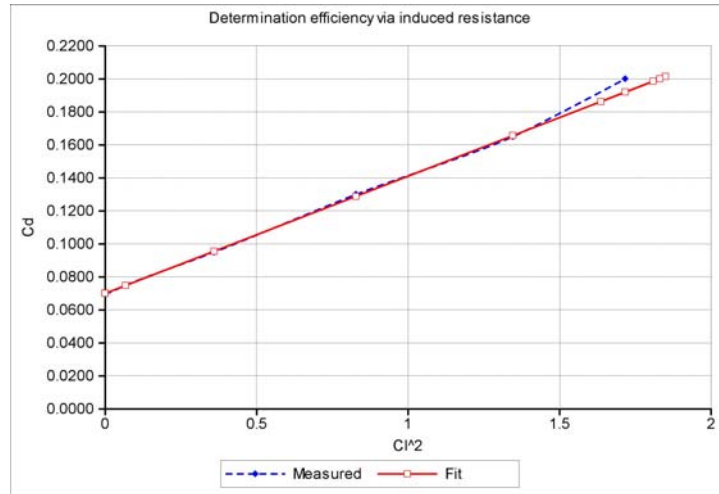


Figure 9 Determination of effective aspect ratio

The quadratic separation drag is given by:

$$C_{ds} = 0.016C_l^2 \quad (17)$$

And finally the remaining part of the drag C_{d0} can be found by subtracting the induced drag and the quadratic separation drag from the measured drag that in turn was already corrected with the bare poles measured data. The values for C_{l0} and C_{d0} are tabulated for a range of apparent wind angles. In the VPP use is made of interpolation to find the correct values. After this the other drag components are computed and added to the interpolated aerodynamic drag.

5.3. Windage

The windage has been subtracted from the measured data. In general due to scale effects (mostly Reynolds effects) the windage measured in the wind tunnel is too high and is therefore discounted from the measured data.

In the VPP the drag due to hull and rigging is determined as follows:

$$\begin{aligned} C_{dhull} &= 0.764 fva^2 \left(B_{oa} \left[0.5 \cos(\alpha') + 0.5 \right] + L_{oa} \sin(\alpha') \right) \cdot \left(EHH \cos(\varphi) + B_{oa} / 2 \sin(\varphi) \right) / A_{ref} \\ C_{drigging} &= 1.1 \cdot A_{rigging} / A_{ref} \end{aligned} \quad (18)$$

The first equation is adapted from Hansen et al. (2002). In this equation fva is the speed reduction from the center of effort height to the half hull height due to the assumed wind gradient and α' the apparent wind angle at the hull. EHH is the effective height of the hull and B_{oa} and L_{oa} are the overall width and length of the hull. $A_{rigging}$ is the combined area of all rigging. In this case only the mast has been included, as it was assumed that the bare sail coefficients already took most of the other drag components into account.

The effect of heeling is for these relatively wide and shallow boats very large and has been included in the windage.

Center of effort height

The height of the center of effort is determined in a simplified manner, taking into account the geometric dimensions of the sails, the windage and the relative loading of the various windage components.

6. VELOCITY PREDICTION PROGRAM

6.1. General approach

The velocity prediction program integrates the resistance model, the stability, and the aerodynamic model. The VPP presented here is built along the lines of the VPP as described by Kerwin (1975) and by Claughton et al. (1998).

In synthesis it works as follows:

1. A true wind velocity and true wind angle are assumed. Based on an assumed boat speed the apparent wind velocity and direction can be found.
2. The aerodynamic model (section 5) is used to find the heeling force and driving force due to the combined sail forces and influence of the hull and rigging.
3. The heeling force causes a heeling moment that is balanced by the stability. Using the curve of arms of stability (section 4) the resulting heeling angle can be found.
4. The heeling angle influences the center of effort height and thus the apparent wind velocity and angle and moreover has an influence on the profile of the sails. Steps #2-#4 are repeated until a consistent heeling force and heeling angle are found.
5. Now the resistance is calculated at the assumed boat speed. The resistance is found using the resistance model (section 3) and is composed of:
 - a. Upright viscous and residuary hull resistance, both dependent on the boat speed.
 - b. The change of hull resistance due to heel; again split in a residuary and a viscous part. These components are dependent on the boat speed and heeling angle.
 - c. The change of hull resistance due to trim, dependent on the trimming moment and the boat speed.
 - d. Induced resistance, dependent on boat speed, heeling angle, leeboard position, and magnitude of the side force.
 - e. The appendage resistance. The rudder resistance is included in the upright hull resistance. Remaining is the part of leeboard resistance that is not included in the induced resistance.

This part consists for the most part of viscous resistance and dependent on the boat speed and the leeboard position.

6. The resistance is compared to the driving force. The boat speed is adjusted until the driving force equals the resistance. Generally this velocity will divert from the assumed velocity in step #1 and the whole process is continued until the velocity calculated in step #6 equals the velocity used in step #2.

6.2. Optimizations

For the velocity iteration a bisection method has been employed to enhance the stability of the iteration.

Moreover a scheme has been implemented to control the heeling angle. A so-called reefing angle is preset. When the heeling angle increases beyond this reefing angle a depowering scheme is invoked, using reef and flat parameters to reduce the sailing forces until the heeling angle is below the threshold set by the reefing angle. When the iteration results in the boat speed, the reefing angle is increased and the procedure is repeated until the boat speed starts decreasing or when the reef and flat parameters become unity. Now it is assumed that the optimum boat speed and heeling angle at this wind angle and speed has been found. This scheme is in accordance with the work of Kerwin (1975).

The reef and flat parameters have been incorporated as follows:

$$C_{d0} = reef^2 C_{d0} + reef^2 flat^2 C_{ds} + reef^2 flat^2 C_{di} + C_{dw} \quad (19)$$

$$C_{l0} = C_{l0} reef^2 flat$$

In the VPP it has been assumed that the reefing is preset in the input by specifying a sail set for each wind speed. For this reason the reef parameter is only allowed to operate in narrow band from 0.9 to 1.0. The flat parameter is allowed to operate in a much broader band. In practice flat was never found to be smaller than 0.85.

Figure 10 shows the influence of the reef and flat parameters along with the preset reefing on the lift and drag coefficients of the sails. The continuous line represents the original sailing model. The circles represent the sail model as used for low wind velocities (4 m/s). Clearly no reef and flat is used in this case. The crosses show the sail model as used for higher wind velocities (9 m/s). In this case the reefing is preset and shows as a reduction of both the lift and drag for all apparent wind angles. The flat parameter is used for apparent wind angles below 50 degrees and shows as a clear reduction of the lift and a slight reduction of the drag.

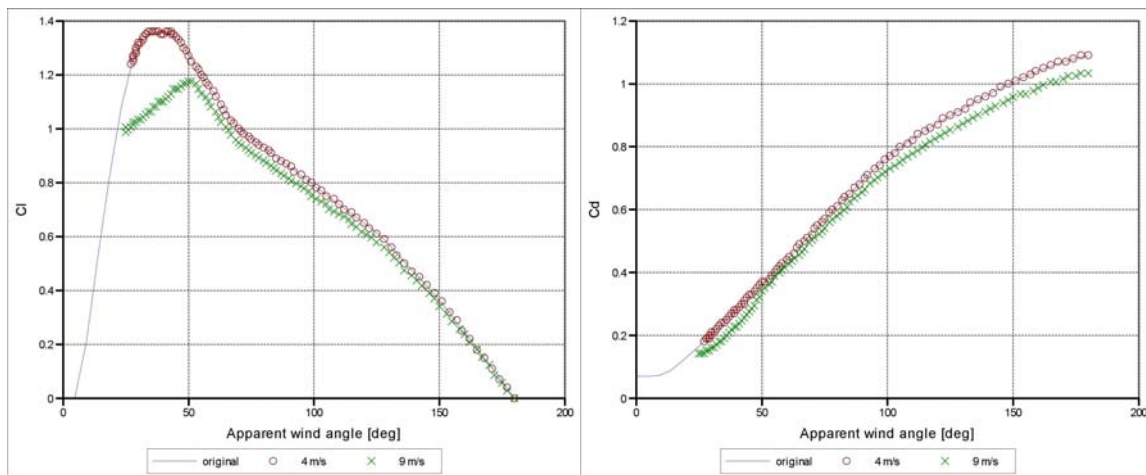


Figure 10 Influence of reefing and flat on the lift (left) and drag (right) coefficients of the sails

Additionally, the VPP calculates the optimum speed made good.

6.3. Input and output

The input to the VPP consists of the true wind velocities and angles, the main dimensions of the ship and sails and of control parameters for the VPP.

The output consists of polar plots and hydromechanic and aerodynamic force tables. Besides that, the VPP is capable of producing the results of the boat on a predefined race course in terms of sailing time and velocity on each leg of the course. The latter data can be used to compare the performance of different boats.

Figure 11 shows a typical polar plot

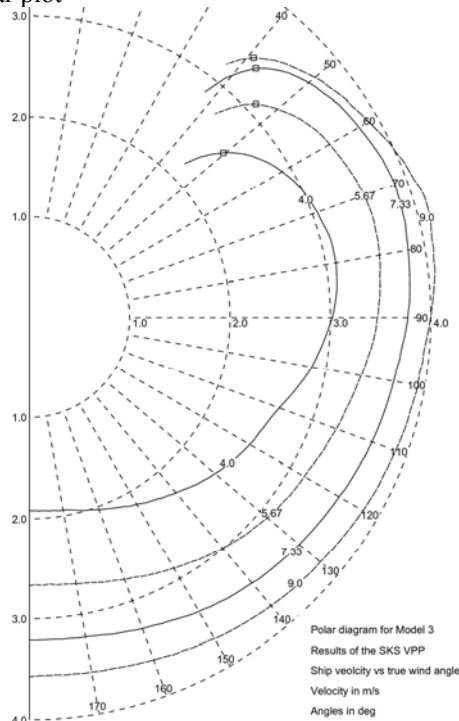


Figure 11 Polar plot Model 14 based on true wind velocity and angle

7. RESULTS

7.1. Comparison of the sailing performance

To compare the performance of the 14 skütsjes the results of the VPP have been used to calculate the sailed time on racing course at four different wind velocities, ranging from 4 m/s (3 Bft) to 9 m/s (5-6 Bft). The course selected was the course of the race at Terherne in the Sneekermeer as used in the 2007 season. The course depicted in Figure 12 had an hourglass shape. The top and bottom legs of the course were aligned with the wind, requiring the boats to tack; both diagonal legs were running courses. Table 2 shows more detailed data of the course.

| Wind direction | 229 | Deg | |
|----------------|---------|-----------------|--------|
| leg | course | true wind angle | Length |
| 1 | tacking | 0.7 deg | 1363 m |
| 2 | running | 156 deg | 1315 m |
| 3 | tacking | 0.6 deg | 1318 m |
| 4 | running | 160 deg | 1570 m |
| total | | | 5567 m |

Table 2 Data of the racing course

The performance on the adverse wind courses was calculated by using the speed made good, while the performance on the running courses was calculated using the polar data at the true wind angle of the course. The performance over the complete course was expressed in terms of sailing time per nautical mile. Table 3 shows the averaged values for each wind velocity.



Figure 12 Construction of the racing course

| Wind velocity | sec/n.m. |
|---------------|----------|
| [m/s] | [1/kts] |
| 4.0 | 1003 |
| 5.7 | 754 |
| 7.3 | 642 |
| 9.0 | 597 |

Table 3 Seconds per nautical mile for four true wind velocities

Clear is the relative slower reduction of sailed time per mile when the wind speed increases. Two effects play a role here. First, due to the reduced water depth the ship resistance increases greatly when the boat speed increases. At the highest wind velocity the boat speed is around 4 m/s, which means a Froude number over the water depth of 0.80. At this Froude number shallow water effects will play an important part in the resistance. Secondly, due to relatively low stability the boats will need to use a reduction of sailing area at the higher wind velocities to avoid excessive heeling or capsizing, having consequences for the boat speed.

Figure 13 shows the deviations of the time per nautical mile from the average time per nautical over all boats per ship in percentages. The top figure shows the values averaged over the four wind velocities. The middle figure shows the values for the lowest wind velocity and the bottom figure for the highest wind velocity. The order of the boats is arbitrary and not equal to Table 1. A positive deviation means a slower ship. Clear is that the maximum difference between the ships is around 4% in terms of seconds per mile. This equals around 40 seconds per mile for the lowest wind velocity and around 25 seconds for the highest wind velocity. Both equal around 4 boat lengths per sailed mile.

Figure 14 shows the deviations of the average speed made good on the left hand side and the deviations of the average boat speed for the running courses on the right hand side. The top figures represent low wind velocity and the bottom figures the high wind velocity. A positive deviation means a faster ship.

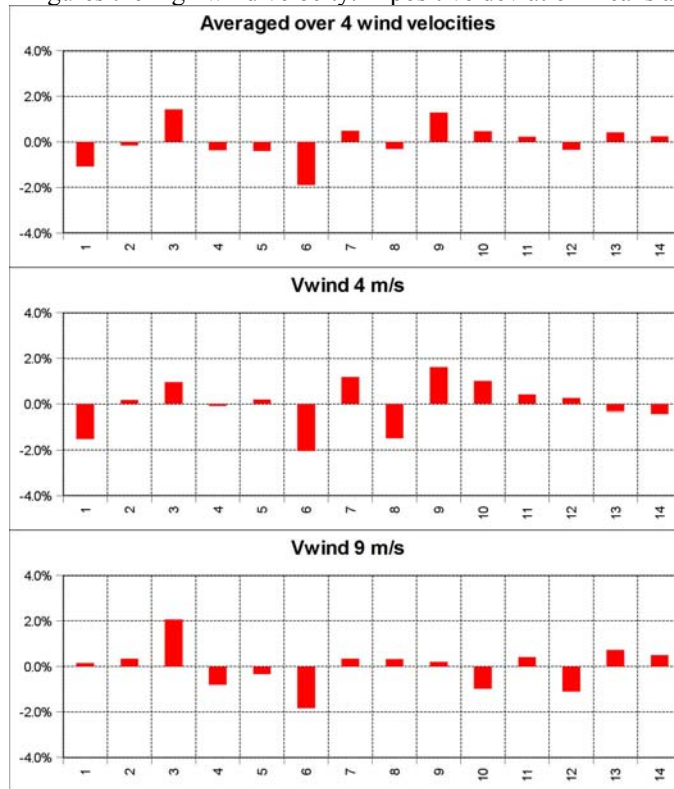


Figure 13 Comparison of deviations of sailed time per mile (positive: slower ship)

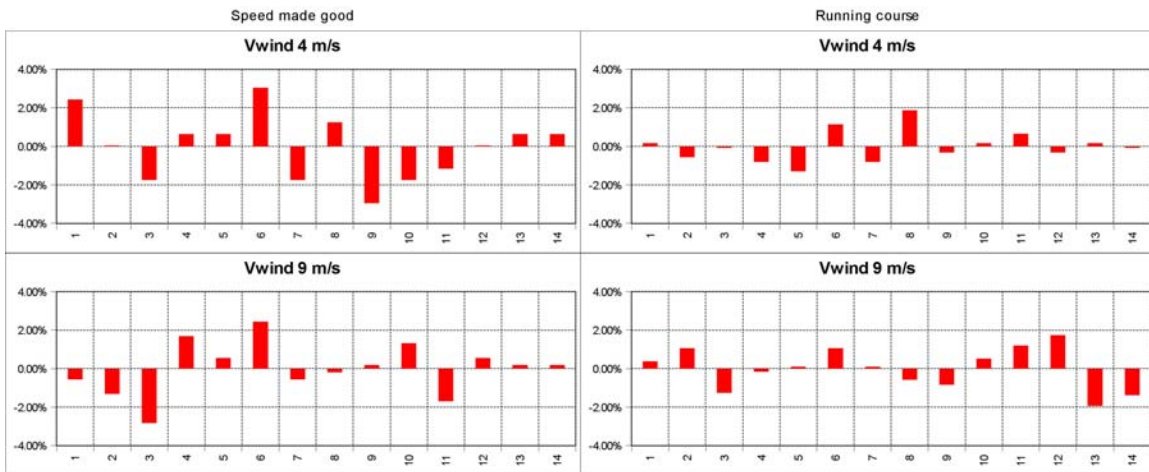


Figure 14 Comparison of deviations of the speed made good and the running speed (positive: faster ship)

It is apparent that the most important differences, up to 6 %, in boat performance are found in the speed made good, while the differences in performance for running courses are limited to maximum 3.5%. Clearly, the highest gains are made when tacking and the differences between the ships are less critical for the performance on running courses.

When studying Figure 13 and Figure 14 it stands out that there are ships that perform better at low wind velocities and have a degrading performance when the wind velocity increases, for instance numbers 1 and 2, and the other way around, like number 7 and 9. Boat numbers 1 and 2 have a relatively low stability,

while numbers 7 and 9 have a much higher stability. This could partly explain the differences found between these boats. For when the wind velocity increases the stability becomes increasingly important to counteract the increasingly higher heeling moment. Boats with relatively low stability have more difficulties in counteracting the heeling moment and need to reduce the sailing forces much earlier, leading to a reduced performance at higher wind velocities.

7.2. Comparison sailing time difference in real life and according to the VPP

When observing the data from real sailing races a typical difference between the fastest and the slowest ship is 10 to 15 minutes for a race that lasts typically 2 hours. The VPP predicts in similar circumstances maximum 4% difference between fastest and slowest ship, which comes down to around 5 minutes. Disregarding the simplifications made in the model and the fact that the model is not aimed at predicting the absolute performance, this would mean that around a third to a half of the performance differences between the ships can be explained with the technical differences between the ships, while the remaining part can be attributed to differences in skill of the teams and the fact that the VPP neglects interaction effects between the boats and maneuvering.

8. CONCLUSIONS

The setup of a velocity prediction program for traditional Dutch sailing vessels of the type skûtsje has been detailed in this paper. The aim of this VPP is to verify the handicap rule currently employed by the race organizer (the SKS) and when necessary to provide a means to setup a new handicap system. The background of the three main parts of the VPP, the resistance model, the aerodynamic model, and the stability, has been detailed and the inner workings and optimizations of the VPP have been described.

Results have been shown for the performance comparison of the 14 skûtsjes of the SKS fleet. A maximum performance difference between slowest and fastest boat has been found of around 4% in terms of seconds per nautical mile. This means about 4 ship lengths difference per sailed mile. The predicted differences are compared to the differences occurring in real life sailing races with the same boats and are found to be of the same order of magnitude, being around a third to a half of these differences. The remaining difference can be attributed to crew skill and the fact that interaction effects between the boats and maneuvering are neglected.

In conclusion it can be stated that the newly developed VPP is found to be suitable to quantify the performance differences between the boats it is aimed for and in such way can be used as a tool to verify and when necessary improve the handicap rule used by the SKS. It is emphasized that the VPP is specifically aimed at quantifying performance differences between the skûtsjes and not at providing an absolute estimate of the performance of individual boats. For such estimated would require a much higher level of attention to the details of each boat, outside of the scope of this research.

It should be noted that this VPP contains force models especially tailored and suited for the 14 SKS skûtsjes and care should be taken when the VPP is applied to ships of different hull form and sail plan and outside of the parameter range of the 14 SKS skûtsjes.

ACKNOWLEDGEMENT

This research has been commissioned by the Kenniscentrum Jachtbouw of the Noordelijke Hogeschool Leeuwarden with support of the Sintrale Kommisje Skûtsjesilen, the Province of Fryslan and the Samenwerkingsverband Noord-Nederland (the Northern Netherlands Provinces).

REFERENCES

1. Cloughton, R.A. Sheno, and J.F. Wellicom. *Sailing Yacht Design - Theory*. Addison Wesley Longman, WEGEMT, 1998.
2. Larsson, L. and R.E. Eliasson. *Yacht Design*. Adlard Coles Nautical, London, 1994.
3. Indesteege, R.M.L. *Prestatieberekningen van zeilschepen*, Afstudeerwerk TUDelft, Rapportnr. 833-S, 1989.

4. Kerwin, J.E., *A Velocity Prediction Program for Ocean Racing Yachts*, Report 78-11, Department of Ocean Engineering, Massachusetts Institute of Technology, 1975.
5. Gerritsma, J., Onnink, R. and Versluis, A., “Geometry, resistance and stability of the Delft Systematic Yacht Hull Series” *7-th HISWA Symposium*, 1981, Amsterdam
6. Gerritsma, J. and Keuning, J.A., “Performance of Light- and Heavy-displacement Sailing Yachts in Waves”, *The 2nd Tampa Bay Sailing Yacht Symposium*, St. Petersburg, 1988.
7. Keuning, J.A., Onnink, R., Versluis, A. and Van Gulik, A., “The Bare Hull Resistance of the Delft Systematic Yacht Hull Series”, *International HISWA Symposium on Yacht Design and Construction*, Amsterdam RAI, 1996
8. Keuning, J.A. and Binkhorst, B.J., “Appendage Resistance of a Sailing Yacht Hull”, *13th Chesapeake Sailing Yacht Symposium*, 1997
9. Keuning, J.A. and Sonnenberg, U.B., “Approximation of the Hydrodynamic Forces on a Sailing Yacht based on the Delft Systematic Yacht Hull Series”, *International HISWA Symposium on Yacht Design and Construction*, Amsterdam RAI, 1998.
10. Rae, W.H. and Pope, A., *Low-Speed Wind Tunnel Testing*, Second Edition, John Wiley and Sons, New York, 1984.
11. Wagenaar, M. *Rompvorm en stabiliteitsmeting veertien SKS skûtsjes*. Rapportnr. 07.216, Annmar Engineering, Kraggenburg, 2008.